SSRG International Journal of Mechanical Engineering
ISSN: 2348-8360/ https://doi.org/10.14445/23488360/IJME-V13I8P101

Volume 13 Issue 8, 1-9, August 2026
© 2026 Seventh Sense Research Group®

Original Article

Tensile Properties of Friction Stir Welded AA6061-T6 Aluminum Alloy with Different Tool Geometries and Process Parameters

Ngoc-Tuan La[1], Hong-Ngoan Nguyen[2], Ky-Thanh Ho[3]

[1]*Faculty of Mechanical Engineering, Vinh University of Education Technology, Nghe An, Vietnam.*
[2]*Faculty of Mechanical and Automobile Engineering, Vinh University of Education Technology, Nghe An, Vietnam.*
[3]*Faculty of Mechanical and Automobile Engineering, Thai Nguyen University of Technology, Thai Nguyen, Vietnam.*

[3]*Corresponding Author : hkythanh@tnut.edu.vn*

Received: 22 April 2026 Revised: 23 June 2026 Accepted: 15 July 2026 Published: 27 August 2026

Abstract - *This study analyses the influence of tool pin geometry and process parameters on the friction stir welding process using AA6061-T6 aluminum alloy. The experiments were conducted with varies tool rotational speeds, transverse speeds, and two types of tool pin geometry. Welded products then used for visual analysis in tension measurement for comparing. Results from the experimental revealed that increasing the transverse speed enhances both tensile strength and welded joints' ductility. For the tool geometries, square pin produced higher tensile strength and joint efficiency than the taper-threaded pin. However, at higher transverse speeds, the taper-threaded pin exhibited greater elongation, which is likely attributed to enhanced helical material flow during the welding process. Factorial analysis indicated that transverse speed was the most influence factor affecting ductility, whereas the combined effects of rotational speed and transverse speed affect the joint efficiency. Results of the present research demonstrate that higher transverse speeds provide high joint efficiency and good ductility. These findings extend the practical processing window for friction stir welding of AA6061-T6 aluminum alloy and provide useful guidance for process optimization in industrial applications.*

Keywords - *Friction Stir Welding, Aluminum alloy, Rotational speed, Transverse speed, Pin geometry, Joint efficiency.*

1. Introduction

Due to their high mechanical strength, aluminum alloys are widely used in engineering applications. However, also due to the low melting point, joining these types of materials using conventional methods such as fusion welding becomes challenging. Previous studies indicate the presence of defects such as porosity and degradation of mechanical properties in these alloys during heat-treatment operations [1, 2]. To overcome these limitations, different joining methods, including Friction Stir Welding (FSW), were developed as an effective alternative [3]. This process uses a rotating non-consumable tool to generate frictional heat at the tool-workpiece interface and soften the weld material. The stirring action of the tool also promotes plastic flow and dynamic recrystallization in the weld zone. Since the process operates below the melting temperature of the base material, it can avoid fusion-related defects such as solidification issues [4, 5], distortion, defects, and even degraded mechanical properties [6, 7]. Previous studies have demonstrated that FSW is suitable for joining aluminum alloys [6, 8]. Research on FSW has shown the successful application in dissimilar material systems, including steel-Al, Ti-Al, and Mg-Al alloys [9-12].

Due to the favorable mechanical properties and broad applicability in aerospace, automotive, marine, and structural components, AA6061 is one of the most widely used materials [13, 14]. Despite these advantages, its weldability is limited for conventional fusion, including solidification cracking and reduced joint strength [15]. With the use of the FSW technique, high-quality AA6061 joints can be produced [13], which became the basis for further studies focusing on factors affecting overall performance in FSW of this material type.

In FSW, weld quality is influenced by both process parameters and tool geometry [16]. Previous studies have investigated the effects of process parameters on the welding of AA6061-T6 aluminum alloy, including tool rotational speed, transverse speed, tool geometry, and tool tilt angle [8, 17-21]. Among these factors, rotational speed and transverse speed are the primary factors governing heat generation, heat dissipation, and material flow of the welding process.

A combination of high rotational speed and low transverse speed increases the heat input, promoting plastic deformation and grain refinement within the stir zone [13].

This is an open access article under the CC BY-NC-ND license (http://creativecommons.org/licenses/by-nc-nd/4.0/)

However, excessive heat also accelerates the dissolution of strengthening precipitates, resulting in local softening and mechanical property reduction in the welded joint. Hence, balancing heat generation and material flow is essential for producing high-quality joints. Since the material temperature during FSW can reach approximately 80-90% of the melting point of the base material, ensuring thermal conditions in material softening and flow behavior during the process is very important [18]. Previous studies have employed only low transverse speeds (typically below 110 mm/min) combined with moderate rotational speeds (600-1450 rpm) to maintain an appropriate thermal balance and ensure sound joint formation [8, 17-21].

Besides the process parameters, tool pin geometry also plays a significant role in controlling material flow and determining joint quality. Different pin profiles generate distinct material flow patterns, leading to different local mechanical behaviors at the joints [17, 19, 20]. For example, square pins enhance the stirring action and improve material mixing, whereas threaded pins facilitate uniform material transport within the stir zone. These differences directly influence defect formation, microstructural evolution, and the mechanical performance of the joint.

Previous studies revealed that dynamic recrystallization and grain refinement in the stir zone are closely associated with the mechanical properties of joints [20], indicating that microstructural evolution serves as the critical link between welding conditions and joint performance. Although tool geometry has only a limited influence on the peak welding temperature, it substantially affects material flow behavior and, consequently, the tensile properties of the welded joints [21].

Therefore, weld quality is governed not only by the thermal field but also, and more importantly, by the characteristics of material flow during the welding process. In addition to rotational speed and transverse speed, the tool tilt angle also contributes to material flow and joint consolidation. An appropriate tilt angle enhances the forging action of the tool shoulder, improving material compaction behind the tool and reducing the likelihood of internal defects such as voids and tunnel defects [13, 18].

However, compared with rotational speed and transverse speed, the influence of the tilt angle is generally secondary and is typically optimized within a relatively narrow range. The previous studies on FSW of AA6061-T6 only investigated relatively low welding (transverse) speeds, while the behavior of FSW joints under higher transverse-speed conditions, particularly in terms of joint efficiency and ductility, has received limited attention. Moreover, the combined effects of process parameters and tool pin geometry at elevated welding speeds have not been systematically investigated. This lack of understanding limits the ability to simultaneously optimize welding productivity and mechanical performance for industrial applications.

This study analyses the combination effects of tool rotational speed, transverse welding speed, and tool pin geometry on the mechanical performance of FSW joints for AA6061-T6. The analysis data included transverse welding speeds of up to 315 mm/min. Two types of pin geometries were used and compared to clarify the interactions among the process parameters and evaluate the feasibility of simultaneously achieving high joint efficiency and improved ductility under high-speed welding conditions.

2. Material and Methods

2.1. Experiment Setup

The welding tool consisted of a shoulder and a pin. In this study, two pin geometries were employed: a taper-threaded pin and a square pin, as presented in Figure 1(a). The shoulder had a concave profile, which helps contain the plasticized material and reduce flash formation, thereby improving material flow stability [20, 22].

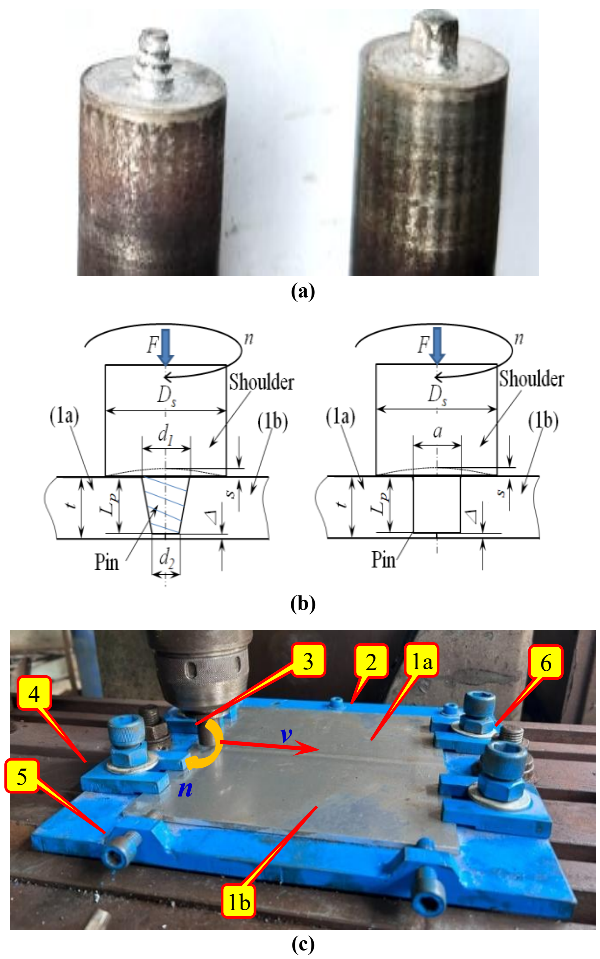

Fig. 1 Experimental setup, (a) Welding tools, (b) Tool dimensions, and (c) Setup on the milling machine, (1) Workpieces, (2) Fixture, (3) Tool, (4) Clamping plates, (5) Bolts, (6) Fixing bolts.

Table 1. Geometrical dimensions of the welding tools used in this work

Tool type	**Geometrical dimensions (mm)**					
	D_s	d_1	d_2	a	L_p	s
Taper-threaded pin	18	3.0	3.0	–	3.8	0.5
Square pin	18	–	–	4.2	3.8	0.5

Table 2. Chemical composition of AA6061 alloy [23]

Element	**Al**	**Si**	**Mg**	**Cr**	**Cu**	**Fe**	**Ti**	**Zn**	**Mn**
Wt (%)	Bal.	0.4-0.8	0.85-1.2	0.04-0.35	0.15-0.4	0.7	0.15	0.25	0.15

Table 3. Typical mechanical properties of AA6061 alloy

Yield strength (MPa)	**Ultimate tensile strength (MPa)**	**Percentage Elongation (%)**	**Hardness (HRB)**
248	301	12.5	55

The geometries of the tools are displayed in Figure 1(b), and their main dimensions are listed in Table 1. The experiments were conducted on a universal milling machine (model 2UMB, Niigata, Japan), as depicted in Figure 1(c).

The workpieces were rigidly fixed on a designed fixture using clamping plates and additional bolts to ensure proper alignment and contact along the joint line. During welding, the rotating tool was plunged into the joint and held for a short dwell time to generate sufficient heat. The tool then traversed along the joint, completing the welding process.

2.2. Preparing Material

The materials of the experiment are 4 mm-thickness AA6061-T6 aluminum alloy plates, whose dimensions are 200x400 mm. The chemical composition of the alloy is presented in Table 2 according to published data [23]. The mechanical properties of the base material, obtained from tensile testing, are listed in Table 3.

2.3. Experiment Design

Based on the experimental setup, a full factorial design was created to evaluate the effects of key process parameters on FSW joints. Three factors were considered, including rotational speed (n), transverse speed (v), and pin geometry (P). The rotational speed was set at two levels (870 and 1240 rpm), while the transverse speed was varied at four levels (80, 125, 200, and 315 mm/min). Two pin geometries were examined: a square pin and a taper-threaded pin (see Figure 1(a)). In total, 16 experimental conditions were set. To improve reliability, each experiment was repeated three times, resulting in 48 tensile specimens. The experimental runs were conducted in a randomized order to reduce potential bias. Table 4 presents the standard and randomized run sequences.

The Ultimate Tensile Strength (UTS) was selected as the primary response and measured in accordance with ASTM E8/E8M-13 [24]. Joint efficiency (E) was subsequently calculated based on the UTS ratio between the welded joint and the base material.

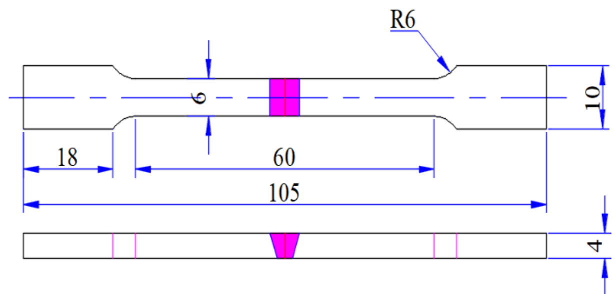

Fig. 2 Tensile specimen geometry [24]

The tensile specimens were prepared such that the loading direction was perpendicular to the welding direction (Figure 2). Percentage elongation (δ) at fracture was recorded to assess ductility. The data were analyzed using Analysis of Variance (ANOVA) to determine the significance of the main factors and their interactions. Main effect and interaction plots were used to examine the influence of the process parameters and pin geometry on the tensile behavior of FSW AA6061-T6 joints.

3. Results and Discussion

3.1. Visual Inspection

The welded joints were first inspected visually. Surface quality, weld continuity, and macroscopic defects like voids or excessive flash were evaluated. In general, the weld surfaces were smooth and continuous, with only limited flash formation. No visible cracks or surface voids were observed. These results confirm that the selected parameters yielded sound joints. Surface morphology is mainly influenced by transverse speed (Figure 3). For a given transverse speed, the surface appearance remains similar regardless of pin geometry. At lower transverse speeds, smoother surfaces are obtained. Higher transverse speeds tend to generate more pronounced surface features. Moreover, differences in flash formation were clearly observed. Welds fabricated with the concave shoulder exhibited a lower amount of flash along the weld edges, which may be attributed to improved material containment beneath the tool.

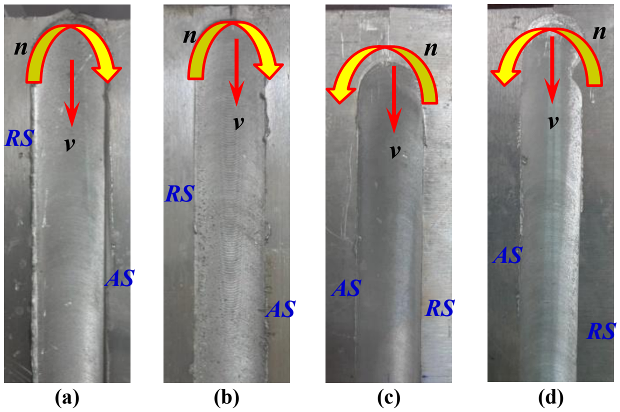

Fig. 3 Visual inspection of weld surfaces under different process conditions, (a) Square pin (n = 1240 rpm, v = 80 mm/min), (b) Square pin (n = 1240 rpm, v = 315 mm/min), (c) Taper-Threaded pin (n = 870 rpm, v = 80 mm/min), and (d) taper-threaded pin (n = 1240 rpm, v = 80 mm/min).

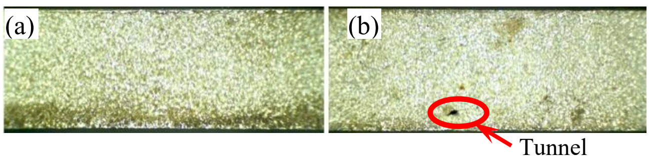

Fig. 4 Cross-Sectional views of FSW joints (without etching) under different process conditions, (a) Square pin (n = 1240 rpm, v = 315 mm/min), and (b) Taper-Threaded pin (n = 1240 rpm, v = 200 mm/min).

Typical cross-sectional views of the welded joints, observed without etching, are provided in Figure 4. For the square pin at a rotational speed of 1240 rpm and a transverse speed of 315 mm/min (Figure 4(a)), the weld cross-section appears continuous and of good integrity, without internal voids or tunnels. On the contrary, the weld produced by taper-threaded pins at 1240 rpm and 200 mm/min exhibits a distinct tunnel defect (Figure 4(b)). It indicates that the outer surface appearance can not guarantee defect-free welding joints.

3.2. Tensile Testing Results

Table 4 presents the measured Ultimate Tensile Strength (UTS, MPa), joint efficiency (E, %), and percentage elongation (δ, %) of the products from the full factorial design, according to rotational speed, transverse speed, and pin geometry. The highest tensile strength was 278.8 MPa, corresponding to a rotational speed of 1240 rpm and a transverse speed of 315 mm/min using the square pin, with a joint efficiency of 92.6%. This result is consistent with previous studies, indicated that square pins can promote stable material flow and fine-grain structures [25]. On the other hand, the specimen using the taper-threaded pin at 870 rpm and 125 mm/min has the lowest tensile strength (191.5 MPa, corresponding to 63.6% efficiency). This reduction in strength likely results from insufficient material flow or inadequate heat input for material flow and recrystallization in welding area.

The table shows that square pin produces higher tensile strength and joint efficiency, particularly at higher rotational speeds. Transverse speed also has a high influence on mechanical performance, where higher speeds (200–315 mm/min) improve local strength and lower transverse speeds (80 mm/min) reduce strength and ductility. The elongation of the specimen after the process ranges from 3.6% to 7.7%, indicating a strong dependence on both pin geometry and process parameters. For higher transverse speeds, the taper-threaded pin exhibits improved elongation. This behavior can be attributed to enhanced material flow along the threaded profile, which facilitates uniform plastic deformation. It also supports the previous findings, which reported that threaded pins not only enhance material flow but also facilitate uniform plastic deformation [26].

Two distinct fracture modes were observed, as illustrated in Figure 5. Some specimens fractured near the weld center, while others failed in the region adjacent to the tool shoulder. The fracture location depends on both process parameters and pin geometry. Fracture at the weld center is typically linked to internal defects such as voids or tunnel defects (Figure 4(b)).

Alternatively, failure near the shoulder region appears to be governed by local softening caused by thermal effects during welding. This difference is also reflected in Table 4. Specimens containing internal defects exhibit lower strength, whereas those fractured near the shoulder region generally show higher ductility.

Table 4. Average tensile strength, joint efficiency, and percentage elongation of FSW joints

Std_Order	Run_Order	*n* (rpm)	*v* (mm/min)	Pin geometry	*UTS* (MPa)	*E* (%)	*δ* (%)
2	1	870	80	Square	239.4	79.5	4.9
10	2	1240	80	Square	219.9	73.1	4.5
4	3	870	125	Square	212.2	70.5	4.0
15	4	1240	315	Taper-threaded	236.2	78.5	7.7
5	5	870	200	Taper-threaded	214.1	71.1	4.5
14	6	1240	200	Square	255.5	84.9	4.1
1	7	870	80	Taper-threaded	202.5	67.3	3.6
3	8	870	125	Taper-threaded	191.5	63.6	4.0
12	9	1240	125	Square	240.7	80.0	6.1
7	10	870	315	Taper-threaded	231.6	76.9	5.8

13	11	1240	200	Taper-threaded	233.0	77.4	6.3
9	12	1240	80	Taper-threaded	247.6	82.3	6.1
16	13	1240	315	Square	278.8	92.6	6.5
8	14	870	315	Square	229.1	76.1	6.4
6	15	870	200	Square	236.1	78.4	5.5
11	16	1240	125	Taper-threaded	234.7	78.0	5.7

(a)
(b)
(c)
(d)

Fig. 1 Representative tensile specimens after fracture under different welding conditions, (a) Square pin (n = 870 rpm, v = 80 mm/min), (b) Taper-Threaded pin (n = 870 rpm, v = 125 mm/min), (c) Square pin (n = 870 rpm, v = 315 mm/min), and (d) Square pin (n = 1240 rpm, v = 315 mm/min).

3.3. Effects of Pin Geometry and Process Parameters on Joint Efficiency and Ductility

As shown in Figure 6(a), increasing the rotational speed from 870 to 1240 rpm enhances heat generation. This improves material softening and consolidation, resulting in higher joint efficiency. The effect of transverse speed is non-linear. At low transverse speed (80 mm/min), excessive heat input may degrade mechanical properties due to microstructural coarsening [8]. At an intermediate speed (125 mm/min), insufficient material flow can result in incomplete bonding and internal defects. When the transverse speed increases to 315 mm/min, a better-balanced condition between heat input and material flow is achieved, resulting in improved joint integrity. A similar trend was reported in previous studies, where higher transverse speeds led to improved joint efficiency under comparable conditions [21].

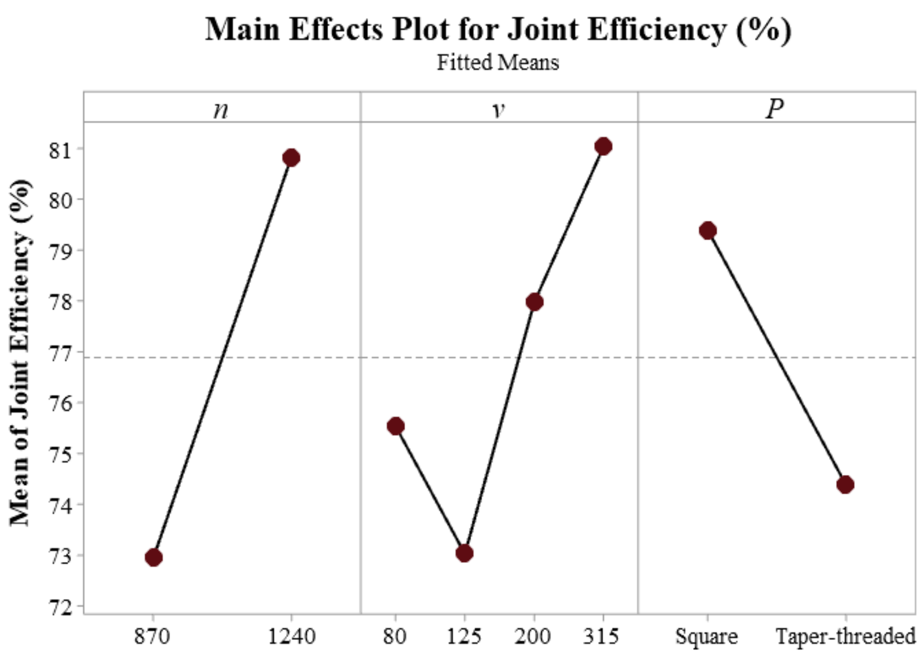

(a)

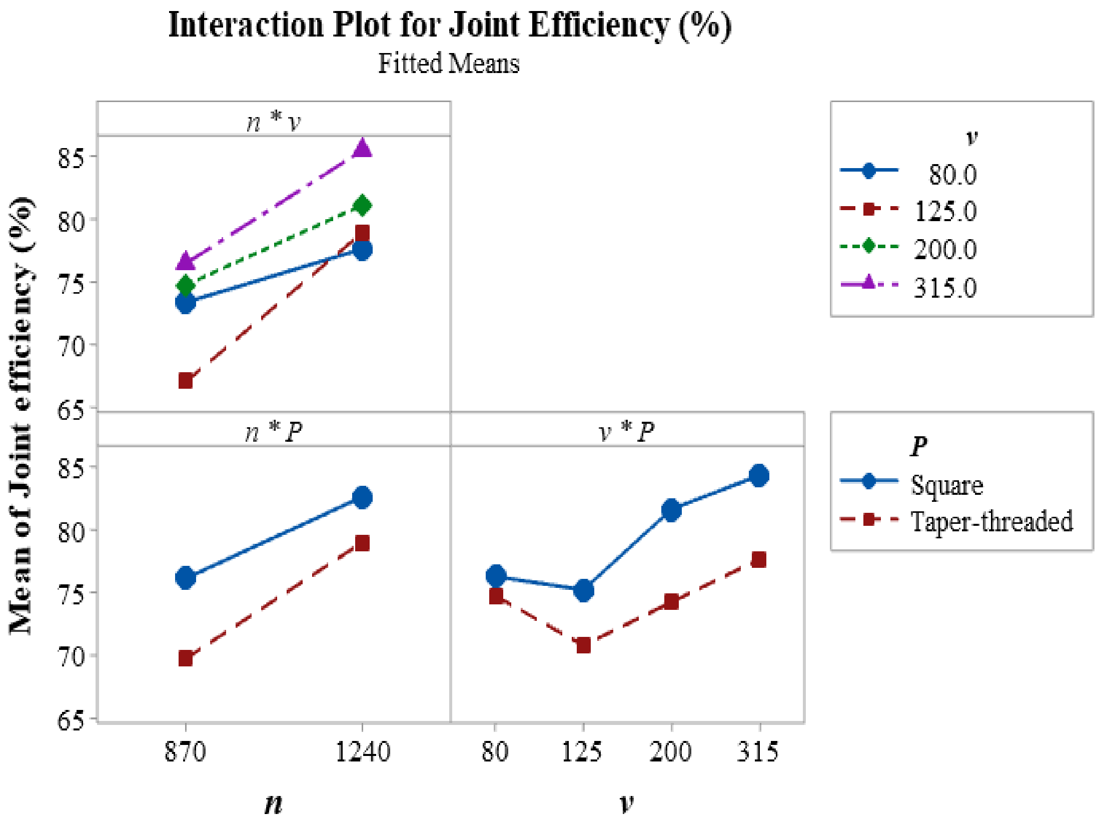

(b)

Fig. 6 (a) Main effects plot the joint efficiency, and (b) Interaction plot for the joint efficiency.

The effect of transverse speed is more pronounced at higher rotational speeds (Figure 6(b)). This suggests a strong coupling between thermal input and material flow. Additionally, higher joint efficiency is consistently observed with the square pin across the investigated conditions, reflecting more effective material mixing [27]. The ANOVA results in Table 5 identify rotational speed (33.7%), transverse speed (19.0%), and pin geometry (13.6%) as the primary contributing factors, with a notable three-way interaction (22.9%). The high determination coefficient (R^2 = 97.5%) indicates the correlation between the regression model and the experimental data. Especially, the contribution of the three-factor combination is higher than that of pin geometry and transverse speed, which presents a strong connection between process parameters and tool design in determining joint efficiency.

Table 5. ANOVA results for joint efficiency

Factor	F-value	p-value	Contribution (%)
Rotational speed (*n*)	431.05	0.000	33.7
Transverse speed (*v*)	81.14	0.000	19.0
Pin geometry (*P*)	173.61	0.000	13.6
$n \times v$	18.94	0.000	4.4
$n \times P$	13.40	0.001	1.0
$v \times P$	12.04	0.000	2.8
$n \times v \times P$	87.84	0.000	22.9

Results from Figure 7 indicate that elongation, as ductility's characteristic, is more influenced by transverse speed than joint efficiency. When the transverse speed increases, ductility rises. The influence of rotational speed also quite clear. This is due to the thermal reduction exposure at higher transverse speeds preserving deformation capacity [28].

Pin geometry plays a more noticeable role in ductility at elevated transverse speeds. Higher elongation is observed with the taper-threaded pin, particularly at 315 mm/min. This behavior reflects more uniform material flow, reducing strain localization in the stir zone. The interaction plot (Figure 7(b)) shows that the effect of transverse speed on elongation is stronger at higher rotational speeds.

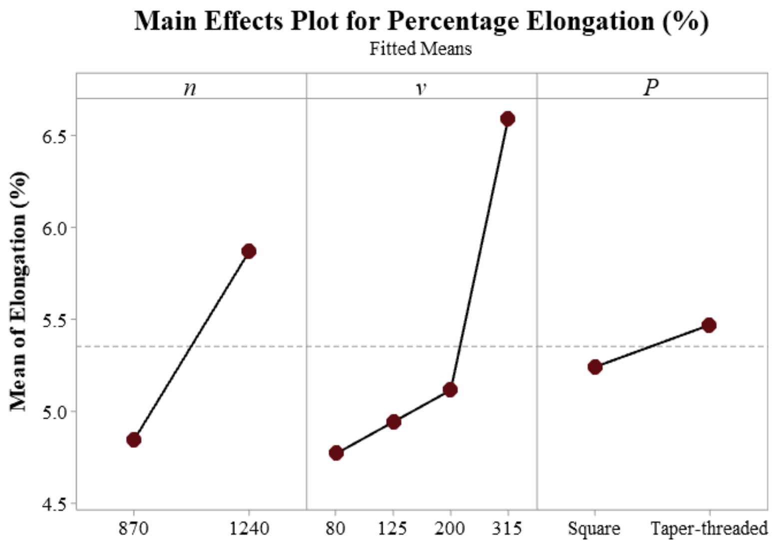

(a)

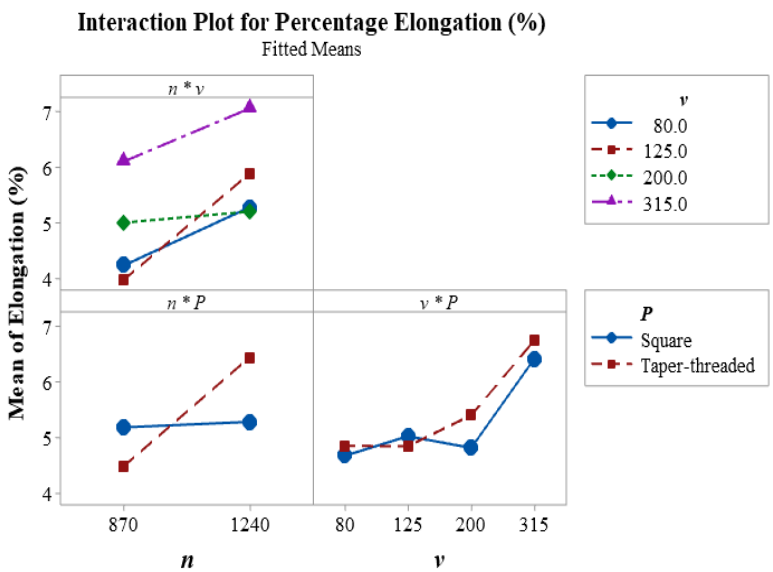

(b)

Fig. 7 Main effects plot, (a) Main effets interaction plot for percentage elongation, and (b) Interaction plot fot percentage elongation.

Table 6 presents the ANOVA results for elongation analysis. According to the table, transverse speed (39.4%) is the most influential factor, followed by rotational speed (19.8%) and the n × P interaction (16.2%). The interaction of three factors (9.6%) also contributes significantly (9.6%), whereas pin geometry has the least effect (1.0%). It is shown that elongation is primarily governed by transverse speed and its interactions with other parameters. The statistical analysis identifies rotational speed, transverse speed, and the n × P interaction as significant factors (p-value < 0.05), while the v × P interaction is not significant (p-value = 0.063). The regression model for elongation yields an R^2 value of 94.3%, revealing a good fit to the experimental data. The taper-threaded pin enhances material flow and ductility; however, its individual contribution remains limited (1.0%), and its effect is mainly manifested through interactions with rotational and transverse speeds.

The observed mechanical trends can be reasonably interpreted in terms of heat input and material flow, although no direct microstructural observations were conducted. Higher rotational speeds increase heat generation, which promotes material softening and consolidation.

Higher transverse speeds reduce thermal exposure, which benefits ductility. The different responses of the two pin geometries arise from their distinct material flow characteristics. The square-shaped pin provides a higher material mixing rate. In contrast, the taper-threaded pin promotes more uniform plastic deformation.

Table 6. ANOVA results for percentage elongation

Factor	F-value	p-Value	Contribution (%)
Rotational speed (n)	111.17	0.000	19.8
Transverse speed (v)	73.68	0.000	39.4
Pin geometry (P)	5.51	0.025	1.0
$n \times v$	12.90	0.000	6.9
$n \times P$	90.61	0.000	16.2
$v \times P$	2.69	0.063	1.4
$n \times v \times P$	17.92	0.000	9.6

The efficiency and ductility of joints exhibit the interaction between processing parameters. Joint efficiency increases with rotational speed but non-linearly changes with transverse speed. Elongation improves when transverse speed increases. Higher transverse speeds can enhance ductility without compromising the strength of the weld. The square pin increases joint efficiency, while the taper-threaded pin is effective in improving ductility. This underscores the need to select an appropriate pin geometry for specific requirements. These findings offer a basis for optimizing the trade-off between strength and ductility in FSW of AA6061-T6.

4. Conclusion

Friction stir welding of AA6061-T6 joints was investigated using square and taper-threaded pins at rotational speeds of 870 and 1240 rpm and transverse speeds ranging from 80 to 315 mm/min. The results show that increasing rotational speed enhances tensile strength due to increased heat input and improved material plasticization. Transverse speed also plays a key role, with higher speeds generally improving both strength and ductility.

Tool geometry affects the mechanical response in different ways. The square pin produces higher tensile strength and joint efficiency. By contrast, higher elongation at elevated transverse speeds is observed with the taper-threaded pin, likely due to improved material flow along the threaded profile. Unlike previous studies focusing on lower transverse speeds, the present results demonstrate that higher transverse speeds can maintain high joint efficiency. Higher transverse speeds also improve ductility, thereby expanding the applicable processing window for AA6061-T6. Depending on application requirements, pin geometry can be selected to prioritize either strength or ductility.

Several limitations should be noted. The investigation was limited to a narrow range of process parameters and only two pin geometries. In addition, no microstructural characterization was performed, which restricts direct correlation between mechanical properties and underlying metallurgical mechanisms.

Future studies should extend the parameter range, examine additional pin geometries, and incorporate detailed microstructural analysis. Evaluation of fatigue behavior and fracture toughness is also necessary to assess the performance of FSW joints.

Conflicts of Interest

The authors declare that there is no conflict of interest regarding the publication of this paper.

Funding Statement

This research received no external funding.

Acknowledgments

The authors gratefully acknowledge the support of Thai Nguyen University of Technology, Thai Nguyen, Vietnam in conducting this research.

References

[1] Sampurna Patnaik, Somnath Chattopadhyaya, and Sachindra Shankar, “Friction Stir Welding and its Applications: An Overview,” *AIP Conference Proceedings: 3rd International Conference on Energy and Power*, Chiang Mai, Thailand, vol. 2681, no. 1, pp. 1-9, 2022. [CrossRef] [Google Scholar] [Publisher Link]

[2] D.A.P. Prabhakar et al., “A Review of Optimization and Measurement Techniques of the Friction Stir Welding (FSW) Process,” *Journal of Manufacturing and Materials Processing*, vol. 7, no. 5, pp. 1-56, 2023. [CrossRef] [Google Scholar] [Publisher Link]

[3] Noah E. El-Zathry et al., “Friction Stir-Based Techniques: An Overview,” *Welding in the World*, vol. 69, no. 2, pp. 327-361, 2025. [CrossRef] [Google Scholar] [Publisher Link]

[4] Ky-Thanh Ho et al., “An Experimental Study on the Tensile Strength of Friction Stir Welded AA5052 Aluminum Alloy,” *Proceeding of 5th International Conference on Advances in Manufacturing and Materials Engineering*, Kuala Lumpur, Malaysia, pp. 389-395, 2023. [CrossRef] [Google Scholar] [Publisher Link]

[5] A.W. El-Morsy, M. Ghanem, and H. Bahaitham, “Effect of Friction Stir Welding Parameters on the Microstructure and Mechanical Properties of AA2024-T4 Aluminum Alloy,” *Engineering, Technology & Applied Science Research*, vol. 8, no. 1, pp. 2493-2498, 2018. [CrossRef] [Google Scholar] [Publisher Link]

[6] Mohamed M.Z. Ahmed et al., "Friction Stir Welding of Aluminum in the Aerospace Industry: The Current Progress and State-of-the-Art Review," *Materials* vol. 16, no. 8, pp. 1-33, 2023. [CrossRef] [Google Scholar] [Publisher Link]
[7] Mostafa Akbari et al., "Recent Advances in Friction Stir Welding/Processing Tools," *Journal of Manufacturing Processes*, vol. 142, pp. 99-156, 2025. [CrossRef] [Google Scholar] [Publisher Link]
[8] Virendra Pratap Singh et al., "Effect of Rotational Speed on Mechanical, Microstructure, and Residual Stress Behaviour of AA6061-T6 Alloy Joints through Friction Stir Welding," *Journal of Materials Engineering and Performance*, vol. 33, pp. 3706-3721, 2024. [CrossRef] [Google Scholar] [Publisher Link]
[9] Y.R. Gunjal et al., "Friction Stir Welding of Dissimilar Metals: Investigating the Role of Interlayers in Aluminium-Steel Butt Joint Performance," *Materials Today Communications*, vol. 50, pp. 1-16, 2026. [CrossRef] [Google Scholar] [Publisher Link]
[10] Mian Wasif Safeen, and Pasquale Russo Spena, "Friction Stir Welding of Aluminum Alloys and Steels: Issues and Solutions," *Characterization of Minerals, Metals, and Materials 2019*, pp. 189-200, 2019. [CrossRef] [Google Scholar] [Publisher Link]
[11] Wenjing Yang et al., "Improve the Impact Property in a Novel Butt Joint of Ti/Al Dissimilar Metals," *Heliyon*, vol. 10, no. 14, pp. 1-6, 2024. [CrossRef] [Google Scholar] [Publisher Link]
[12] Mohammad Pervez Mughal, Amir Nawaz, and Syed Farhan Raza, "Friction Stir Welding of Magnesium AZ31B and Aluminum Al-6062," *Advances in Manufacturing Technology XXXV*, pp. 135-142, 2022. [CrossRef] [Google Scholar] [Publisher Link]
[13] B.T. Ogunsemi et al., "A Review of Various Improvement Strategies for Joint Quality of AA 6061-T6 Friction Stir Weldments," *Journal of Materials Research and Technology*, vol. 11, pp. 1061-1089, 2021. [CrossRef] [Google Scholar] [Publisher Link]
[14] Vishnu Venugopal, Virendra Pratap Singh, and Basil Kuriachen, "Underwater Friction Stir Welding of Marine Grade Aluminium Alloys: A Review," *Materials Today: Proceedings*, 2023. [CrossRef] [Google Scholar] [Publisher Link]
[15] Ali Jalili et al., "Pre-Weld Friction Stir Processing Mitigates Hot Cracking and Strengthens AA6061 Fusion Welds," *Scientific Reports*, vol. 15, pp. 1-10, 2025. [CrossRef] [Google Scholar] [Publisher Link]
[16] Mohamed M.Z. Ahmed et al., "Review on Friction Stir Welding of Dissimilar Magnesium and Aluminum Alloys: Scientometric Analysis and Strategies for Achieving High-Quality Joints," *Journal of Magnesium and Alloys*, vol. 11, no. 11, pp. 4082-4127, 2023. [CrossRef] [Google Scholar] [Publisher Link]
[17] Chetan Chalurkar, and Dinesh Kumar Shukla, "Temperature Analysis of Friction Stir Welding (AA6061-T6) with Coupled Eulerian-Lagrangian Approach," *IOP Conference Series: Materials Science and Engineering: International Conference on Materials Science and Engineering*, vol. 1248, pp. 1-14, 2022. [CrossRef] [Google Scholar] [Publisher Link]
[18] Abhijit Banik et al., "An Experimental Investigation of Torque and Force Generation for Varying Tool Tilt Angles and their Effects on Microstructure and Mechanical Properties: Friction Stir Welding of AA 6061-T6," *Journal of Manufacturing Processes*, vol. 31, pp. 395-404, 2018. [CrossRef] [Google Scholar] [Publisher Link]
[19] Wasif Safeen et al., "Predicting the Tensile Strength, Impact Toughness, and Hardness of Friction Stir-Welded AA6061-T6 using Response Surface Methodology," *The International Journal of Advanced Manufacturing Technology*, vol. 87, pp. 1765-1781, 2016. [CrossRef] [Google Scholar] [Publisher Link]
[20] Ashu Garg, Madhav Raturi, and Anirban Bhattacharya, "Strength, Failure and Microstructure Development for Friction Stir Welded AA6061-T6 Joints with Different Tool Pin Profiles," *CIRP Journal of Manufacturing Science and Technology*, vol. 29, pp. 99-114, 2020. [CrossRef] [Google Scholar] [Publisher Link]
[21] S. Emamian et al., "Influences of Tool Pin Profile on the Friction Stir Welding of AA6061," *ARPN Journal of Engineering and Applied Sciences*, vol. 11, no. 20, pp. 12558-12261, 2016. [Google Scholar] [Publisher Link]
[22] D. Ambrosio et al., "Material Flow in Friction Stir Welding: A Review," *Journal of Materials Processing Technology*, vol. 320, 2023. [CrossRef] [Google Scholar] [Publisher Link]
[23] Mohammad Inggi Hilmawan et al., "Effect of Tools Rotational Speed on the Mechanical Properties of One-Step Double-Acting Friction Stir Welded Aluminum Alloy AA 6061 Hollow Panel," *International Journal of Lightweight Materials and Manufacture*, vol. 7, no. 3, pp. 467-479, 2024. [CrossRef] [Google Scholar] [Publisher Link]
[24] *E8/E8M − 13a: Standard Test Methods for Tension Testing of Metallic Materials*, ASTM International, pp. 1-28, 2013. [Google Scholar] [Publisher Link]
[25] Gaurav Chauhan et al., "Microstructure Evolution and Recrystallization in Friction Stir Welding Process Analyzed by Material Vorticity," *Welding in the World*, vol. 70, no. 3, pp. 919-934, 2026. [CrossRef] [Google Scholar] [Publisher Link]
[26] Majid Elyasi et al., "The Effect of Pin Thread on Material Flow and Mechanical Properties in Friction Stir Welding of AA6068 and Pure Copper," *Heliyon*, vol. 9, no. 4, pp. 1-14, 2023. [CrossRef] [Google Scholar] [Publisher Link]
[27] Bharat Singh et al., "Role of Various Tool Pin Profiles in Friction Stir Welding of AA2024 Alloys," *Journal of Materials Engineering and Performance*, vol. 30, no. 11, pp. 8606-8615, 2021. [CrossRef] [Google Scholar] [Publisher Link]
[28] Vincenzo Lunetto et al., "A Review of Friction Stir Welding of Industrial Alloys: Tool Design and Process Parameters," *Journal of Manufacturing and Materials Processing*, vol. 9, no. 2, pp. 1-48, 2025. [CrossRef] [Google Scholar] [Publisher Link]